

A differential dielectric spectroscopy setup to measure the electric dipole moment and net charge of colloidal quantum dots

R. J. Kortschot, I. A. Bakelaar, B. H. Erné, and B. W. M. Kuipers

Citation: [Review of Scientific Instruments](#) **85**, 033903 (2014); doi: 10.1063/1.4867666

View online: <http://dx.doi.org/10.1063/1.4867666>

View Table of Contents: <http://scitation.aip.org/content/aip/journal/rsi/85/3?ver=pdfcov>

Published by the [AIP Publishing](#)

Articles you may be interested in

[Fluorescence resonance energy transfer measured by spatial photon migration in CdSe-ZnS quantum dots colloidal systems as a function of concentration](#)

Appl. Phys. Lett. **105**, 203108 (2014); 10.1063/1.4902223

[Effect of metal oxide morphology on electron injection from CdSe quantum dots to ZnO](#)

Appl. Phys. Lett. **102**, 163119 (2013); 10.1063/1.4803173

[Optical susceptibilities in singly charged ZnO colloidal quantum dots embedded in different dielectric matrices](#)

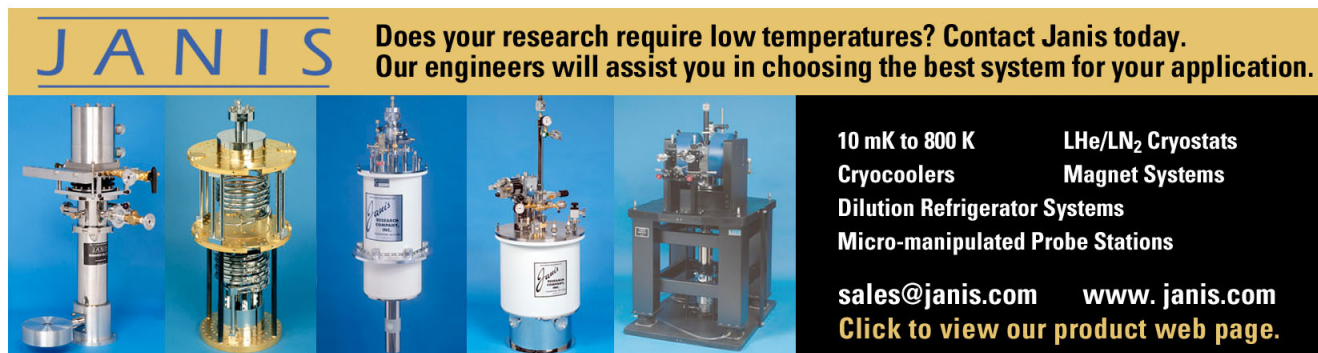
J. Appl. Phys. **113**, 054303 (2013); 10.1063/1.4789363

[Electrically driven light emission from single colloidal quantum dots at room temperature](#)

Appl. Phys. Lett. **90**, 023110 (2007); 10.1063/1.2425043

[Permanent dipole moment and charges in colloidal semiconductor quantum dots](#)

J. Chem. Phys. **111**, 6955 (1999); 10.1063/1.479988



JANIS Does your research require low temperatures? Contact Janis today.
Our engineers will assist you in choosing the best system for your application.

10 mK to 800 K LHe/LN₂ Cryostats
Cryocoolers Magnet Systems
Dilution Refrigerator Systems
Micro-manipulated Probe Stations

sales@janis.com www.janis.com
[Click to view our product web page.](#)

A differential dielectric spectroscopy setup to measure the electric dipole moment and net charge of colloidal quantum dots

R. J. Kortschot, I. A. Bakelaar, B. H. Ern , and B. W. M. Kuipers^{a)}

Van 't Hoff Laboratory for Physical and Colloid Chemistry, Debye Institute for Nanomaterials Science, Utrecht University, Padualaan 8, 3584 CH Utrecht, The Netherlands

(Received 4 December 2013; accepted 23 February 2014; published online 13 March 2014)

A sensitive dielectric spectroscopy setup is built to measure the response of nanoparticles dispersed in a liquid to an alternating electric field over a frequency range from 10^{-2} to 10^7 Hz. The measured complex permittivity spectrum records both the rotational dynamics due to a permanent electric dipole moment and the translational dynamics due to net charges. The setup consists of a half-transparent capacitor connected in a bridge circuit, which is balanced on pure solvent only, using a software-controlled compensating voltage. In this way, the measured signal is dominated by the contributions of the nanoparticles rather than by the solvent. We demonstrate the performance of the setup with measurements on a dispersion of colloidal CdSe quantum dots in the apolar liquid decalin.

  2014 AIP Publishing LLC. [<http://dx.doi.org/10.1063/1.4867666>]

I. INTRODUCTION

Two essential electric properties of colloidal semiconductor nanoparticles, so-called quantum dots, are their net charge and permanent electric dipole moment. They affect their optical properties¹ and colloidal interactions,^{2,3} for instance, enabling controlled assembly of particles on a substrate using electric fields.⁴ The electric properties can be determined from the complex permittivity spectrum when the particles are dispersed in a liquid.^{5,6} Dilute dispersions have the advantage of avoiding interparticle interactions and of limiting the required amount of precious particles, but the relative contribution of the nanoparticle dipole moments to the permittivity spectrum is weak. To optimize sensitivity, we built a complex dielectric spectroscopy setup whose output signal can be nullified in the absence of nanoparticles, so that after they are added to the liquid, their contribution dominates the measured signal.

Both dipole moment and charge of colloidal quantum dots can be determined by dielectric spectroscopy. The permanent electric dipole moment of particles with a hydrodynamic radius on the order of 2–8 nm dispersed in a liquid with a viscosity of about 1 mPa s is observable in the permittivity spectrum as a Debye relaxation in the 10^5 – 10^7 Hz frequency range.^{5,6} Net charge on the particles gives rise to conductivity of the dispersion and polarization of the electrodes,^{6,7} with a relaxation frequency of typically 10^{-1} – 10^3 Hz, a function of cell geometry, ion concentration, and mobility of the charged particles. Both the dipole moment and the net charge can also be measured by other techniques. Dipole moments have been measured using optical spectroscopy⁸ or with transient electric birefringence (for rod-like particles).⁹ Net charges have been determined by transient current analysis¹⁰ and laser Doppler electrophoresis.¹¹ Additionally, it has been shown by electrostatic force microscopy that quantum dots can acquire a net charge upon illumination.¹² Here, by measuring the per-

mittivity spectrum from 10^{-2} to 10^7 Hz using a transparent capacitor, we want to make it possible to measure both the net charge and permanent dipole moment in the dark and under illumination in a single setup.

Dielectric spectroscopy is well-known in soft matter science and has been applied to many materials, for instance, polymers,¹³ proteins,¹⁴ and colloids.¹⁵ Commercial analyzers for dielectric spectroscopy generally include automatic balancing bridges and frequency response analysis.^{16,17} The bridge achieves balance by automatically adjusting capacitive and resistive components,^{18–20} and the permittivity at a particular frequency is calculated from the circuit components in the balanced situation. Phase-dependent voltages are measured using gain-phase analyzers, vector voltmeters, or lock-in amplifiers (LIA). A broad frequency range can be accessed thanks to measurement resistors whose values can be selected on a logarithmic scale.²¹ The end result is the total permittivity of the sample. Our own objective is to measure directly the *excess* permittivity from the differential signal of a bridge circuit. Background signal is removed using a software-controlled phase-dependent compensating voltage.^{22–24} The bridge is balanced on pure solvent, and upon addition of colloidal nanoparticles, the complex excess permittivity is measured at the highest possible sensitivity of the lock-in amplifier.

This paper is organized as follows: the experimental setup is presented in Sec. II, followed by its characterization and calibration in Sec. III. Permittivity spectra are shown in Sec. IV, and conclusions are drawn in Sec. V.

II. EXPERIMENTAL SETUP

A. General principle

The setup consists of a differential impedance bridge in which two capacitors are compared (Fig. 1) to measure the complex excess permittivity $\epsilon^{\text{ex}}(\omega)$

$$\epsilon^{\text{ex}}(\omega) = \epsilon(\omega) - \epsilon_s, \quad (1)$$

^{a)}Author to whom correspondence should be addressed. Electronic mail: B.W.M.Kuipers@uu.nl

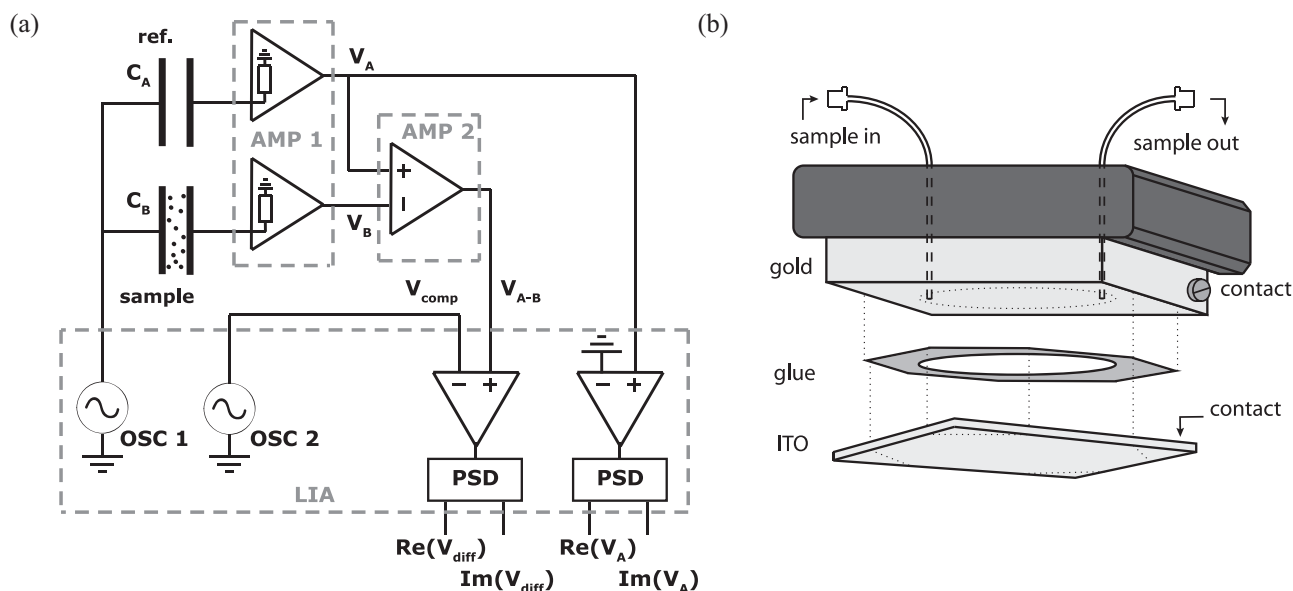


FIG. 1. Schematic diagrams of (a) the differential permittivity measurement circuit and (b) the transparent sample capacitor.

where $\epsilon(\omega)$ is the permittivity of the colloidal dispersion, ϵ_s is the permittivity of the solvent, and $\omega = 2\pi f$ is the angular frequency. Capacitor C_A is a reference capacitor with capacitance C_A or C , and capacitor C_B contains either dispersion or solvent and has capacitance C_B . The voltage V_{A-B} is proportional to the difference ΔC in capacitance between sample and reference capacitors. Ideally, the reference capacity is such that ΔC is zero at each frequency for a background measurement (ΔC_{bg}), i.e., the sample capacitor filled with pure solvent. Then, the excess complex capacitance or permittivity can be measured with a sample measurement (ΔC_s), i.e., the sample capacitor filled with a dispersion. In practice, the bridge is never exactly balanced and ΔC_{bg} is neither zero nor frequency independent. To measure at the highest sensitivity, not limited by any offset, a compensating voltage V_{comp} is applied in both the sample and the background measurements. This is similar to the approach that we followed to develop a differential magnetic susceptibility setup.²² A sample capacitor with one transparent indium tin oxide (ITO) electrode was constructed to allow measurements under illumination.

B. Hardware

The electronics of the setup are a Zurich Instruments HF2LI differential LIA and two external Zurich Instruments HF2CA current pre-amplifiers (AMP1/AMP2). The LIA has two synchronized oscillation outputs (OSC1/OSC2) and two phase sensitive detectors (PSD).

The signals of the reference and sample branches, V_A and V_B , respectively, are measured with the two independent amplification channels of the first amplifier (AMP1), which has a 10^1 – 10^6 Ω selectable measurement resistor. These signals are subtracted using the second amplifier (AMP2), yielding V_{A-B} . A second output (OSC2) is used to apply a complex compensating voltage (V_{comp}), to reduce any offset if the impedance bridge is not perfectly balanced at a particular frequency. This voltage is subtracted from V_{A-B} by the LIA, yielding V_{diff} . The voltage of the reference branch V_A is also

measured separately, providing magnitude and phase of the voltage over the reference capacitor.

The transparent capacitor consists of one gold-plated electrode (25 mm \times 25 mm \times 7.5 mm) and one ITO coated glass electrode (25 mm \times 25 mm \times 1.1 mm, surface resistivity 8–12 Ω /sq, Sigma Aldrich). Both square electrodes are glued together on the edges with adhesive (Araldite, AW2101/HW2951), through which 75 μ m diameter glass spacer beads (Sigma Aldrich) are mixed. Two polytetrafluoroethylene syringe tubes (Sigma Aldrich) are glued in two holes (diameter = 1 mm) through the gold electrode to fill the capacitor with dispersion. Conductive silver epoxy (SPI, #05062) is used for electrical contact with the ITO electrode.

An adjustable capacitor with aluminum electrodes and Teflon spacer was used as reference capacitor. The spacing could be adjusted by varying the distance between the electrodes using screws. The reference capacitor was set equal roughly to the high frequency capacitance of the sample capacitor. Both capacitors were measured independently with an HP4192A impedance analyzer. The circuit was placed in an electrically grounded and thermally insulated box with internal copper walls in contact with copper tubing thermostated using liquid pumped from a Julabo F25 thermostatic bath (± 0.01 $^\circ$ C).

C. Measurement procedure

Determination of the excess capacitance C^{ex} requires measurement of V_{diff} and V_A , both for a sample measurement on dispersion and a background measurement on pure solvent. Additionally, the nullification procedure is necessary to determine and to apply a compensating voltage V_{comp} . All measurement procedures were implemented on a PC using LABVIEW software.

The measurement procedure is as follows. First, the capacitor is filled with a sample and the voltage V_{A-B} is measured directly without compensating voltage, starting with the

least sensitive range of the LIA, and switching successively to more sensitive ranges if no overload is expected.²² Second, a compensating voltage V_{comp} is applied, which is set equal to the measured voltage V_{A-B} , and the remnant signal V_{diff} is measured. Third, since V_{diff} is not necessarily zero, V_{comp} is adjusted by an iterative procedure as discussed below, to further reduce V_{diff} . Finally, the capacitor is filled with pure solvent and, while the optimal V_{comp} is maintained, V_{diff} is measured at the highest sensitivity. Independently from this nullification procedure, the voltage V_A is measured.

The compensating voltage V_{comp} necessary to nullify V_{diff} , in order to reduce any offset, was determined by an iterative nullification procedure that we developed for this setup.²⁴ This procedure rapidly converges to the noise-limited minimum by taking into account the instrumental damping and phase shifting of V_{comp} in terms of an empirical complex constant $\tilde{\alpha}$. According to this procedure, the output of the circuit is determined in the n th step of the iteration by $V_{\text{diff}}^n = V_{A-B} - \tilde{\alpha}^n V_{\text{comp}}^n$. After the initializing step, in which $V_{\text{comp}}^0 = V_{A-B}$, the compensating voltage is then determined by

$$V_{\text{comp}}^{n+1} = \frac{V_{A-B}}{\tilde{\alpha}^n} = \frac{V_{\text{comp}}^n}{1 - (V_{\text{diff}}^n/V_{A-B})}. \quad (2)$$

As explained in Ref. 22, it is preferred to perform the nullification procedure during the sample measurement and to apply the same compensating voltage again during the background measurement, instead of the other way around.

The selectable measurement resistors of AMP1 are chosen to be as large as possible, but with the restriction $\omega RC < 0.015$, where R is the measurement resistance. AC coupling is selected for AMP1 and AMP2 at frequencies above 100 kHz. An oscillating voltage of 1 V was applied, unless stated otherwise. Usually, 10 data points are averaged at each frequency. Calibration of the setup was performed at 22.0 °C with toluene (J.T. Baker), cyclohexane (Interchema), and diethyl ether (Biosolve). Tertbutylammonium tertphenylborate (Fluka) was dissolved in hexanol (Sigma-Aldrich).

D. Calculation of the permittivity

The electric circuit allows calculation of the difference between capacitances, $\Delta C = C_B - C$, by measuring the voltage over the reference resistor, V_A , and the voltage difference between the two resistors, V_{A-B} . In the case of $\omega RC \ll 1$,

$$\Delta C = -C \frac{V_{A-B}}{V_A}. \quad (3)$$

To exclude any additional capacitance resulting from an imperfectly balanced bridge, the increment in capacitance due to the sample is determined from a sample measurement (s, with sample) and a background measurement (bg, without sample)

$$C^{\text{ex}} = \Delta C^{\text{s}} - \Delta C^{\text{bg}} = -C \left(\frac{V_{A-B}^{\text{s}}}{V_A^{\text{s}}} - \frac{V_{A-B}^{\text{bg}}}{V_A^{\text{bg}}} \right) \quad (4)$$

provided that $\omega RC \ll 1$ and $\omega RC \cdot V_{A-B}/V_A \ll 1$.

The nullification procedure applies a compensating voltage to cancel any remaining signal, which is required in the case that the sample signal is smaller than the additional capacitance due to an imperfectly balanced bridge. In this case, one measures $V_{\text{diff}} = V_{A-B} - V_{\text{comp}}$ and C^{ex} is determined from

$$C^{\text{ex}} = -C \left(\frac{V_{\text{diff}}^{\text{s}}}{V_A^{\text{s}}} - \frac{V_{\text{diff}}^{\text{bg}}}{V_A^{\text{bg}}} \right) \quad (5)$$

provided that $\omega RC \ll 1$ and $\omega RC \cdot V_{\text{diff}}/V_A \ll 1$.

Measurements of electrode polarization at lower frequencies require less sensitivity, and alternatively, V_B can be measured directly. In this case, the reference branch is disconnected, and C_B is obtained from

$$C_B = \frac{V_B}{i\omega R V_{\text{app}}} \quad (6)$$

with V_{app} the applied voltage.

The complex excess relative permittivity due to the nanoparticles ϵ^{ex} is given by

$$C^{\text{ex}} = K_c \epsilon^{\text{ex}} \approx \frac{A}{d} \epsilon_0 \epsilon^{\text{ex}} \quad (7)$$

with K_c the cell constant of the capacitor, A the surface area of the capacitor, d the spacing between the capacitor plates, and ϵ_0 the vacuum permittivity.

III. CHARACTERIZATION AND CALIBRATION

The setup is characterized and calibrated with organic solvents of known permittivity and low conductivity. The results are used to determine the cell constant of the capacitor.

The impedance spectra of the transparent capacitor with different solvents (Fig. 2(a)) resemble that of a capacitor and resistor in parallel, though not perfectly. When measured with the differential setup in the 10^2 – 10^7 Hz frequency range with a reference capacitor of 185.4 pF, it becomes clear that $Re(\Delta C)$, the component of ΔC that is in phase with the reference capacitor, is not constant (Fig. 2(b)), but it decreases approximately linearly with the logarithm of frequency. Concurrently, the out-of-phase component $Im(\Delta C)$ is nonzero (Fig. 2(c)). Despite this nonideal behavior, which we ascribe to dissipation of the glue spacer which has an impedance parallel to the sample impedance, accurate measurements are possible. Empirically we find, when calculating the excess capacity C^{ex} compared to toluene, that the capacity scales linearly with the permittivity of the solvents (Fig. 2(d)). $Im(C^{\text{ex}})$ shows effects of nonzero conductivity and approaches zero at higher frequencies (Fig. 2(e)), while above 1 MHz inductive effects become visible, proportional to $Re(C^{\text{ex}})$. To calibrate the setup and to determine the cell constant of the capacitor, $Re(C^{\text{ex}})$ is averaged over the 10^3 – 10^6 Hz frequency range for each solvent and plotted against the relative permittivity of the solvent, known from literature²⁵ (Fig. 2(f)). The slope in this plot is equal to the cell constant $K_c = 28.70 \pm 0.10$ pF. The surface area of the capacitor was determined from a digital photograph of the capacitor ($A = 3.07$ cm²). Using Eq. (7), the distance between the electrodes is estimated to be

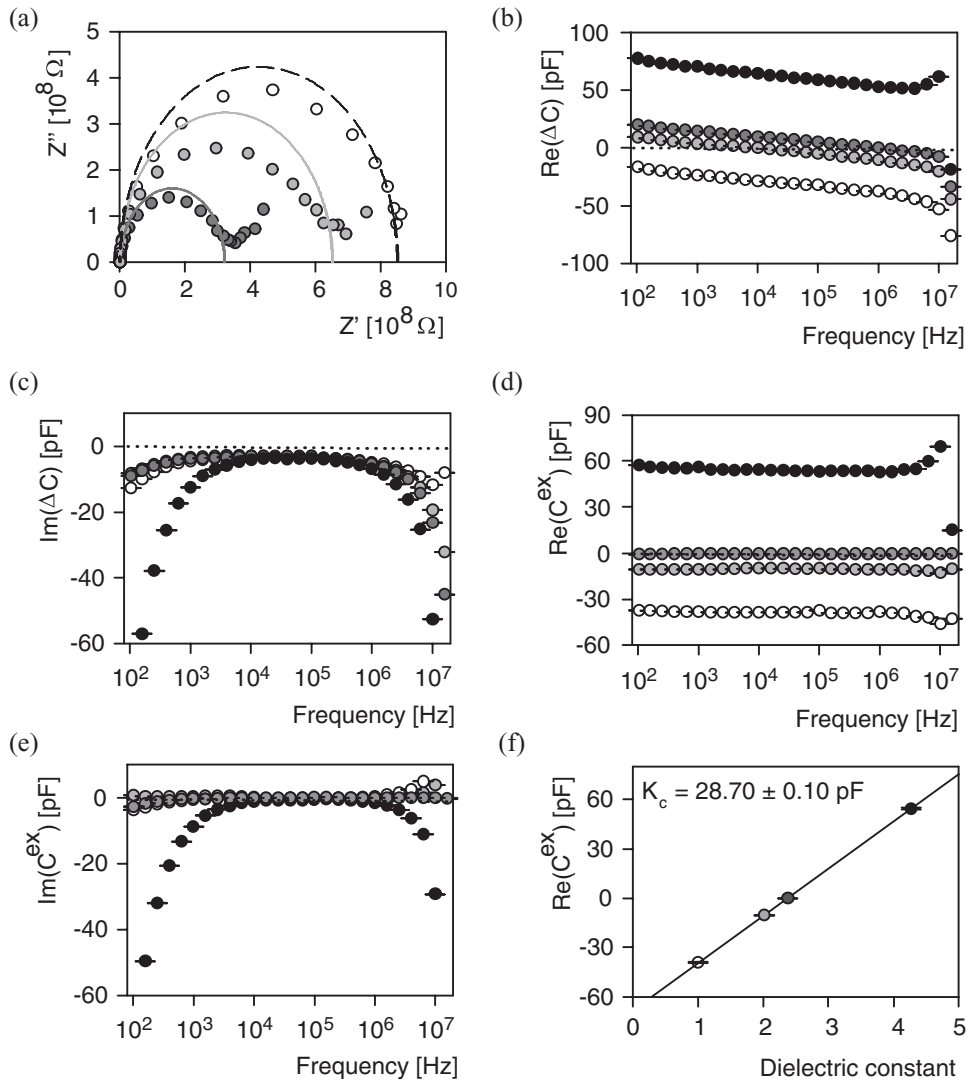


FIG. 2. Calibration in the 10^2 – 10^7 Hz range with different solvents (diethyl ether ●, toluene ○, cyclohexane ◐) and air (○): (a) Impedance spectrum $Z = Z' - iZ''$, (b) $\text{Re}(\Delta C)$, (c) $\text{Im}(\Delta C)$, (d) $\text{Re}(C^{\text{ex}})$, and (e) $\text{Im}(C^{\text{ex}})$ as a function of frequency, and (f) $\text{Re}(C^{\text{ex}})$ as a function of solvent permittivity to determine the cell constant K_c .

$d = 94.6 \mu\text{m}$, slightly larger than the average diameter of the silica glass beads ($75 \mu\text{m}$) used as spacer.

At lower frequencies (10^{-2} – 10^2 Hz), C^{ex} goes up dramatically (Figs. 3(a) and 3(b)), due to electrode polarization. Apparently, charged impurities are present in the solvents, be it at very low concentrations ($\sim\text{nM}$ for diethyl ether, $<\text{nM}$ for toluene and cyclohexane). Calibration with an air capacitor ($C^{\text{ex}} = 900$ pF) shows that our setup operates properly in this frequency range (Fig. 3(c)). No attempts were made to measure at even lower frequencies, despite the hardware low frequency cut-off at $1 \mu\text{Hz}$.

The sensitivity of the setup was probed by measuring the capacitance of two separate aliquots of toluene and comparing the difference C^{ex} . Care was taken to refill the capacitor without disturbing the circuit, and to keep the circuit well thermostated. A resolution down to $\epsilon^{\text{ex}} \approx 10^{-3}$ (corresponding to 0.01% of total capacitance) was achieved in the frequency range of 10^4 – 10^7 Hz (Fig. 4), where dipole relaxations are expected for nanoparticles. A higher resolution is expected to be possible, by reducing the measurement time, which reduces drift.

IV. PERMITTIVITY SPECTRA

As a demonstration of the setup, the excess complex permittivity spectrum (Fig. 5) was measured of a dilute ($5.5 \mu\text{M}/0.1$ vol. % including surfactant shell) dispersion of CdSe quantum dots with a 4.0 nm core diameter dispersed in decalin.²⁶ A Debye relaxation is clearly observed in the 10^4 – 10^6 Hz frequency range due to rotation of the nanoparticles. The expected frequency response of particles with a permanent electric dipole moment μ in the weak field limit is

$$\epsilon_d(\omega) = \frac{\Delta\epsilon_d}{1 + i\omega\tau_d}, \quad (8)$$

where $\Delta\epsilon_d = n\mu^2/(3kT\epsilon_0)$, n is the nanoparticle number density, and τ_d is the Brownian rotation relaxation time

$$\tau_d = \frac{4\pi\eta a_H^3}{kT}, \quad (9)$$

where a_H is the hydrodynamic radius of the nanoparticle, η is the solvent viscosity, k is the Boltzmann constant, and T is the temperature. Here, a relaxation time of $\tau_d = 9.5 \times 10^{-7}$ s corresponds to a hydrodynamic radius of $a_H = 4.3$ nm, in

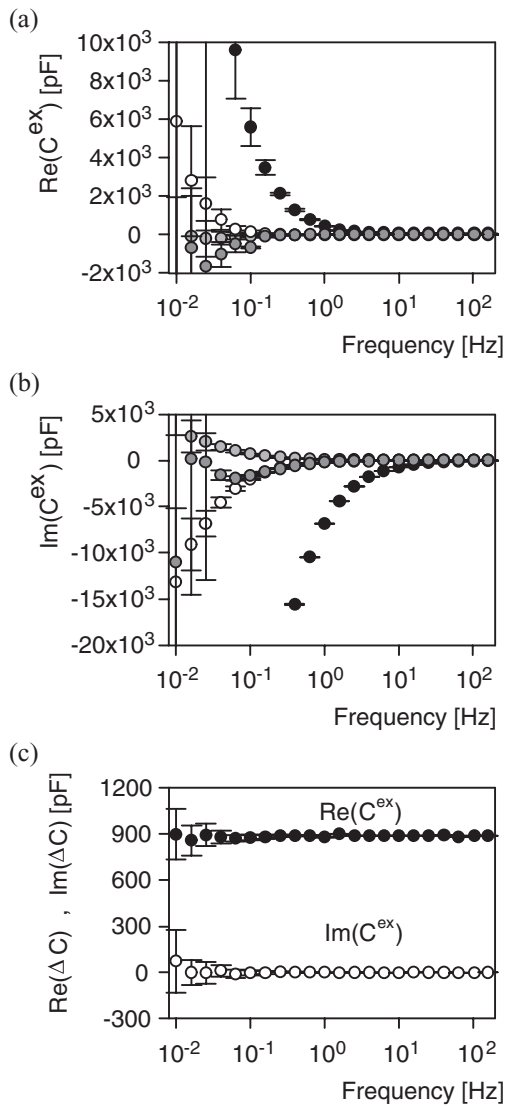


FIG. 3. Calibration in the 10^{-2} – 10^2 Hz range with different solvents (diethyl ether ●, toluene ○, cyclohexane ◊) and air (○): (a) $\text{Re}(C^{\text{ex}})$ and (b) $\text{Im}(C^{\text{ex}})$ as a function of frequency, and (c) calibration with an air capacitor ($C^{\text{ex}} = 900$ pF). The error bars indicate the standard deviation of ten measurements at each frequency.

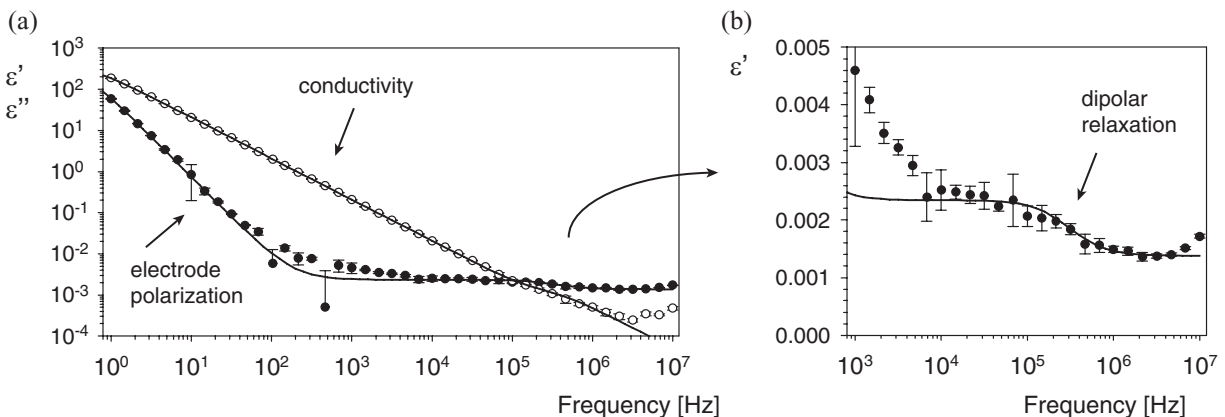


FIG. 5. Excess permittivity (ϵ' : ●, ϵ'' : ○) of a dilute dispersion of CdSe quantum dots in decalin (0.1 vol. %): (a) total spectrum and (b) a close-up of the dipolar relaxation. Solid lines are fits using Eqs. (8) and (10).

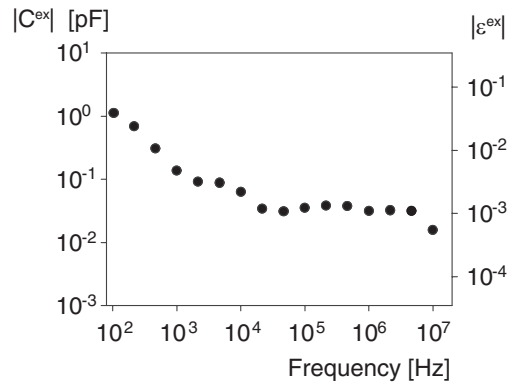


FIG. 4. Differential measurement between two aliquots of toluene.

agreement with the dimensions of the nanoparticle covered with a 2.3 nm oleic acid shell. The magnitude of the relaxation $\Delta\epsilon_d = 0.00097$ yields a dipole moment $\mu = 53$ D, which is close to previously reported values.^{5,6}

The finite conductivity indicates the presence of charged species, which, at low frequencies, leads to electric double layers at the electrodes. The relaxation of these double layers is described by the following function:^{26,27}

$$\epsilon_{\text{EP}}(\omega) = \frac{\Delta\epsilon_{\text{EP}}}{(i\omega\tau_{\infty})^{1-\alpha} + i\omega\tau} \quad (10)$$

in which $\Delta\epsilon_{\text{EP}} = \epsilon_s\kappa d/2$ is the relaxation magnitude, d is the distance between the electrodes, $\tau = d/(2D\kappa)$ is the double layer relaxation time, $\tau_{\infty} = 1/(D\kappa^2)$ is the Maxwell-Wagner relaxation time, and α is an empirical constant. The translation diffusion coefficient of the charged species is $D = kT/(6\pi\eta a_H)$, and the Debye length is $\kappa^{-1} = [\epsilon_0\epsilon_s kT/(2nq^2)]^{1/2}$, where q is the magnitude of the positive and negative charges and $2n$ their total number density. Here, a fit of the electrode polarization yields that a fraction of 1.2% of the nanoparticles carries a net charge of $\pm 1e$, while the other nanoparticles are charge-neutral.

After fitting of the electrode polarization and the dipolar relaxation, a small shoulder is observed in the real part of the permittivity in the 10^2 – 10^4 Hz frequency range. This shoulder is likely an artifact. Exactly in this frequency range the ratio ϵ'/ϵ'' is the smallest ($\epsilon'/\epsilon'' < 0.01$), hence ϵ' is the most

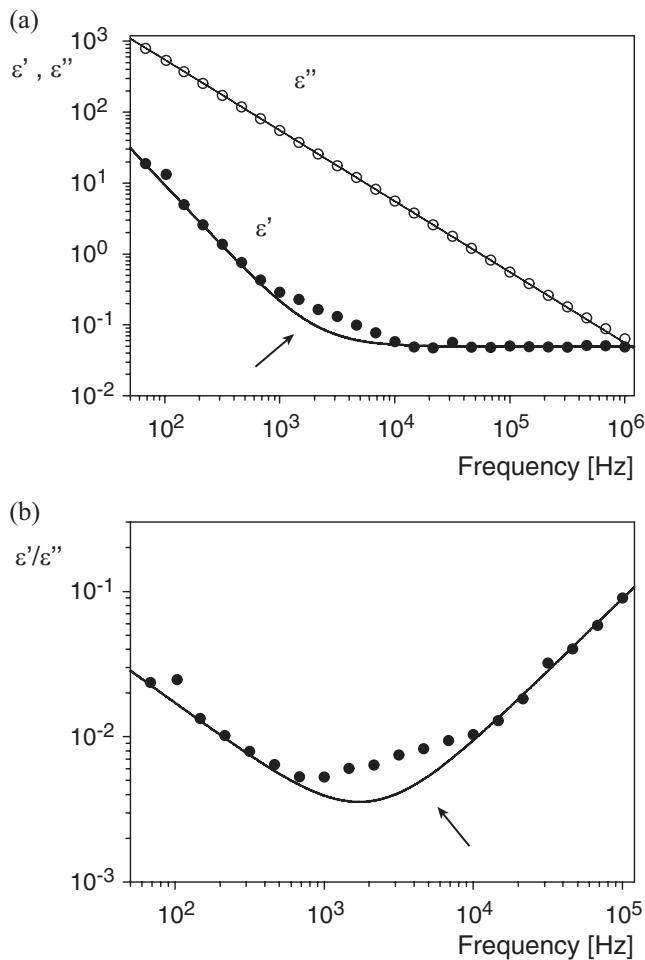


FIG. 6. Permittivity spectrum of tertbutylammonium tertphenylborate salt in hexanol and fitted for electrode polarization. The part of the real permittivity in (a) that is not fitted well, as indicated by the arrow, corresponds to the frequency range where the ratio ϵ'/ϵ'' in (b) is the smallest.

susceptible for, for instance, a small systematic error in the phase angle in the measured impedance. As indicated in Fig. 6, this shoulder is also observed in the permittivity spectrum of tertbutylammonium tertphenylborate salt in hexanol, which does show electrode polarization as well. This shoulder does not obstruct the observation of the dipolar relaxation.

V. CONCLUSIONS

The described setup successfully measures the complex excess permittivity of liquid dispersions of colloidal quantum dots in the 10^{-2} – 10^7 Hz frequency range, using a differential circuit with background compensating voltage. Measurement

on a dilute dispersion of CdSe quantum dots demonstrates sufficient sensitivity to measure the dipolar relaxation due to a permanent dipole moment and the conductivity and electrode polarization due to particles with a net charge.

ACKNOWLEDGMENTS

CdSe quantum dots were kindly provided by Relinde van Dijk-Moes. Ernst van Faassen and Casper van der Wel are acknowledged for useful discussions, and the latter also for providing Fig. 1(b). This work was supported by The Netherlands Organisation for Scientific Research (NWO).

- ¹S. A. Emedocles and M. G. Bawendi, *Science* **278**, 2114 (1997).
- ²M. Klokkenburg, A. J. Houtepen, R. Koole, J. W. J. de Folter, B. H. Ern , E. van Faassen, and D. Vanmaekelbergh, *Nano Lett.* **7**, 2931 (2007).
- ³J. van Rijssel, B. H. Ern , J. D. Meeldijk, M. Casavola, D. Vanmaekelbergh, A. Meijerink, and A. P. Philipse, *Phys. Chem. Chem. Phys.* **13**, 12770 (2011).
- ⁴S. Ahmed and K. M. Ryan, *Chem. Commun.* **2009**, 6421.
- ⁵S. A. Blanton, R. L. Leheny, M. A. Hines, and P. Guyot-Sionnest, *Phys. Rev. Lett.* **79**, 865 (1997).
- ⁶M. Shim and P. Guyot-Sionnest, *J. Chem. Phys.* **111**, 6955 (1999).
- ⁷A. D. Hollingsworth and D. A. Saville, *J. Colloid Interface Sci.* **257**, 65 (2003).
- ⁸V. L. Colvin and A. P. Alivisatos, *J. Chem. Phys.* **97**, 730 (1992).
- ⁹L. S. Li and A. P. Alivisatos, *Phys. Rev. Lett.* **90**, 097402 (2003).
- ¹⁰M. Cirillo, F. Strubbe, K. Neyts, and Z. Hens, *ACS Nano* **5**, 1345 (2011).
- ¹¹E. V. Shevchenko, D. V. Talapin, N. A. Kotov, S. O'Brien, and C. B. Murray, *Nature (London)* **439**, 55 (2006).
- ¹²T. D. Krauss and L. E. Brus, *Phys. Rev. Lett.* **83**, 4840 (1999).
- ¹³J. P. Runt and J. J. Fitzgerald, *Dielectric Spectroscopy of Polymeric Materials* (American Chemical Society, 1997).
- ¹⁴R. Pethig, *Annu. Rev. Phys. Chem.* **43**, 177 (1992).
- ¹⁵A. D. Hollingsworth and D. A. Saville, *J. Colloid Interface Sci.* **272**, 235 (2004).
- ¹⁶F. Kremer and M. Arndt, *Broadband Dielectric Measurement Techniques* (American Chemical Society, 1997), pp. 67–79.
- ¹⁷P. Hedvig, *Dielectric Spectroscopy of Polymers* (Adam Hilger Ltd., Bristol, 1977).
- ¹⁸L. Callegaro, *Instrumentation* **54**, 529 (2005).
- ¹⁹M. Dutta, A. Chatterjee, and A. Rakshit, *Measurement* **39**, 884 (2006).
- ²⁰N. K. Das, T. Jayakumar, and B. Raj, *IEEE Trans. Instrum. Meas.* **59**, 3058 (2010).
- ²¹R. Richert, *Rev. Sci. Instrum.* **67**, 3217 (1996).
- ²²B. W. M. Kuipers, I. A. Bakelaar, M. Klokkenburg, and B. H. Ern , *Rev. Sci. Instrum.* **79**, 013901 (2008).
- ²³“Input offset reduction using the model 7265/7260/7225/7220 synchronous oscillator/demodulator monitor output,” *Signal Recovery*, Technical Report No. AN 1001, 2008.
- ²⁴C. M. van der Wel, R. J. Kortschot, I. A. Bakelaar, B. H. Ern , and B. W. M. Kuipers, *Rev. Sci. Instrum.* **84**, 036109 (2013).
- ²⁵“Permittivity (dielectric constant) of liquids,” *CRC Handbook of Chemistry and Physics*, 93rd ed. 2012–2013 (<http://www.hbcpnetbase.com/>, accessed 2012).
- ²⁶Details of the CdSe quantum dots and further analysis will be presented in a future publication.
- ²⁷J. R. Macdonald, *J. Phys.: Condens. Matter* **22**, 495101 (2010).